Heterogeneous Coverage Control with Mobility-Based Operating Regions

Soobum Kim[1] and Magnus Egerstedt[2]

Abstract— **This paper presents a coverage controller that allows a team of robots with qualitatively different mobility types to achieve an effective coverage over a domain consisting of multiple terrain types. In this work, each robot has specific types of terrains that it can operate on, and these compatible operating regions of a robot are determined based on its mobility type and current position. With the extended definition of coverage from sensing to servicing of events, the Voronoi cells of the robots are confined to their compatible operating regions. Based on the new Voronoi cells, the mobility constrained locational cost is defined, and a gradient descent controller is used to drive robots to locally optimal coverage positions. In order to keep each robot within its compatible regions while achieving a coverage, control barrier functions are utilized.**

I. Introduction

In the field of multi-robot systems, coverage control is a framework to effectively distribute a group of robots over a domain given a profile that describes the relative importance of the points within the domain [1]. In [2], it was shown that the effective distribution of a group of homogeneous robots can be achieved by the continuous time version of Lloyd's algorithm [3] where each robot is driven towards the weighted centroid of its Voronoi cell [4]. Based on this result, cases with heterogeneous robots were considered in the literature. In terms of utilizing heterogeneous sensing capabilities of robots for coverage control, [5], [6], [7] considered robots with different sensing ranges, and [8], [9], [10] examined cases involving robots equipped with multiple types of sensors that can detect different environmental phenomena. From a mobility perspective, [6], [11], [12], [13] studied cases with robots that possess different actuator dynamics. In addition, [14] considered robots with different energy constraints, and [13], [15] investigated cases where robots have different physical dimensions.

The heterogeneity discussed in the preceding works was confined to the robots themselves. Although the robots had different capabilities or characteristics, the domain of interest was implicitly assumed to be comprised of single terrain type. Therefore, every robot in a team could reach the same set of points within the domain. However, in scenarios involving a domain with multiple terrain types and robots with multiple mobility types, each robot may have different regions that they have access to. For example, if a domain of interest consisting of ground and water regions is to be covered with a heterogeneous team of ground and amphibious robots, ground robots only have access to ground regions whereas amphibious robots can operate on both regions. Motivated by this idea, this paper proposes a new coverage controller that achieves an optimal coverage while keeping each robot within their accessible regions in such multi-terrain and multi-species coverage scenarios.

A few studies considered the heterogeneity of the domain to limited degrees. In [16], [17], strategies to achieve static coverage configurations of robots while avoiding collisions with obstacles were proposed. Similarly, [18], [19] discussed how to maintain persistent coverage over a domain with obstacles. These works implicitly embraced the heterogeneity of the domain by restricting access of the robots to areas without obstacles. In [20], a domain was explicitly divided into multiple areas, and each area was selectively covered by a specific type of sensors. However, the sensors in this work did not have any mobility constraints, so any types of sensors could operate on the whole domain.

In contrast to these previous results, this paper considers coverage scenarios where each robot has access to different parts of a domain based on its type and current position. Accordingly, the robots start from their safe operating regions, and they are driven towards optimal coverage locations within the regions. To this end, the domain of interest is categorized into smaller subdomains to identify the accessible domain (safe operating region) of a robot. In this paper, the meaning of coverage is extended to potential servicing of events, i.e., a robot may be required to visit any locations within its region of dominance. Therefore, the Voronoi cell of each robot is restricted to the areas within its accessible domain. The locational cost of the system is redefined with the new Voronoi cells of the robots, and a gradient descent controller is used to drive each robot to locally optimal positions for minimizing the cost. In case of the accessible domain of a robot being non convex, control barrier functions (CBFs) [21] are utilized to keep each robot in their safe operating regions in a minimally invasive manner.

The organization of this paper is as follows. Section II describes the process of categorizing a domain into subdomains to identify accessible domains which are safe operating regions of robots. Based on the accessible domains of robots, the mobility constrained Voronoi cells of robots are defined. In Section III, the locational cost function of the system is redefined with mobility constrained Voronoi cells, and the gradient descent algorithm for the new cost is derived. In Section IV, control barrier functions to keep

This work was supported by the Army Research Lab through Grant No. DCIST CRA W911NF-17-2-0181.

[1]S. Kim is with the School of Electrical and Computer Engineering, Georgia Institute of Technology, Atlanta, GA, USA skim743@gatech.edu

[2]M. Egerstedt is with the Samueli School of Engineering, University of California, Irvine, Irvine, CA, USA magnus@uci.edu

each robot within its safe region is discussed. Section V demonstrates experimental results that show the effectiveness of the proposed controller, and Section VI concludes the paper.

II. Domain Categorization and Mobility Constrained Voronoi Cells

In a coverage scenario involving a domain of interest with multiple terrain types and robots with multiple mobility types, each robot should be operating on its compatible types of terrains. Otherwise, some robots may be damaged either partially or completely. An example of this would be ground robots driven into a river. In order to keep robots within their accessible regions, we first need to define the accessible regions of the robots. To this end, the domain of interest is first categorized into subdomains.

Consider a two dimensional domain $\mathcal{D} \in \mathbb{R}^2$ to cover with a team of robots with different mobility types. The domain is then partitioned into subdomains so that

$$\mathcal{D} = \bigcup_{w=1}^{n_w} \mathcal{D}_w$$

where each subdomain $\mathcal{D}_w$ represents a specific type of terrain within the domain, and $n_w \in \mathbb{N}$ is the total number of subdomains. Also, let $\mathcal{W} = \{1, \cdots, n_w\}$ be the set of the indicies of all subdomains. Since each subdomain represents a type of terrain, the subdomains do not overlap with each other, i.e., $\mathcal{D}_i^\circ \cap \mathcal{D}_j^\circ = \emptyset$, $\forall i, j \in \mathcal{W}$ where $\circ$ notation denotes interior of a set. An example of a domain categorized into subdomains is in Fig. 1 where $\mathcal{D}_1$ and $\mathcal{D}_2$ represent ground and water terrains, respectively. In this case, $n_w = 2$ and $\mathcal{W} = \{1, 2\}$. Note that there are two disconnected ground regions in the example. However, since each subdomain represents a type of terrain, the two disconnected ground regions are classified as $\mathcal{D}_1$, and a water region between the ground regions is classified as $\mathcal{D}_2$.

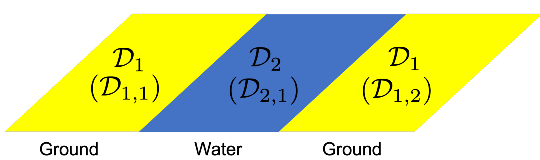

Fig. 1. An example of subdomains and connected subdomains.

Now, let $\mathcal{N} = \{1, \cdots, n\}$ be the set containing the indicies of all robots where n is the total number of robots in the team. The position of Robot i is represented as $p_i \in \mathbb{R}^2$, and the vector containing the positions of all robots is defined as $p = [p_1^\top, \cdots, p_n^\top]^\top$. In addition, let $\mathcal{S} = \{1, \cdots, n_s\}$ be the set containing all types of species, i.e., the types of robots, in the heterogeneous team. Further, let us define a function $s : \mathcal{N} \to \mathcal{S}$ which takes the index of a robot and returns the species of the robot. Consider an example in Fig. 2. If we define 1 as rabbit type and 2 as turtle type, $\mathcal{S} = \{1, 2\}$. The species of a robot with index i can be obtained by plugging the index into the function as $s(i)$. In the example, the species of the robot with index 2 can be found as $s(2) = 2$, which is turtle.

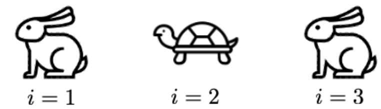

Fig. 2. An example of a robot team consisting of 3 robots in 2 species. The indicies of the robots are shown below them.

Different types of robots may be limited in terms of the types of terrains that they can operate on. For example, consider a case of deploying a heterogeneous team of the rabbit and turtle robots in the domain described in Fig. 1. If we naturally assume that the rabbits are ground robots, and the turtles are amphibious robots, the rabbits can only operate on the regions within the ground subdomain $\mathcal{D}_1$ while the turtles can operate on the whole domain $\mathcal{D}$. We denote the union of subdomains where robots in species $s(i) \in \mathcal{S}$ can operate on as the feasible domain of the species, $\mathcal{F}_{s(i)} \subseteq \mathcal{D}$. Accordingly, the feasible domain of rabbit robots in Fig. 1 is $\mathcal{D}_1$, and that of turtle robots is $\mathcal{D}$.

The subdomains need to be further categorized into smaller regions because there exists an ambiguity if the domain to be covered have disconnected subdomains as $\mathcal{D}_1$ in Fig. 1. Consider a case where a rabbit robot is deployed in the domain described in the figure. If the robot starts from a point within $\mathcal{D}_1$ on the left to the water region $\mathcal{D}_2$, then it only has access to the points within the left part of $\mathcal{D}_1$. Likewise, if the rabbit robot starts from the $\mathcal{D}_1$ on the right to $\mathcal{D}_2$, it only has access to the points within the right part of $\mathcal{D}_1$. In order to distinguish such disconnected subdomains, each subdomain is divided into connected subdomains, as described in the parentheses in Fig. 1. A connected subdomain is denoted as $\mathcal{D}_{w,c}$ where $w \in \mathcal{W}$ is the index of the subdomain that indicates the type of the terrain, and c is the index of the connected subdomain within the subdomain in type w. The connected subdomains satisfy the relationship,

$$\mathcal{D}_w = \bigcup_{c=1}^{C_w} \mathcal{D}_{w,c},$$

where $C_w \in \mathbb{N}$ is the total number of connected subdomains in subdomain w. As an example, in Fig. 1, $\mathcal{W} = \{1, 2\}$, $C_1 = 2$, and $C_2 = 1$.

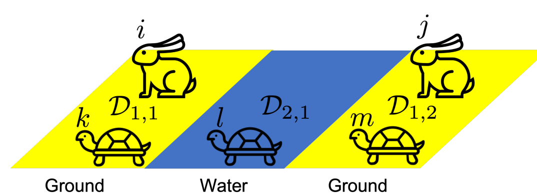

Fig. 3. An example describing two rabbit robots having different accessible domains based on their positions.

Finally, we define the accessible domain of Robot i in species $s(i)$ as $\mathcal{A}_{i,s(i)}(p_i)$, which is the connected subset of

$\mathcal{F}_{s(i)}$ containing the position of Robot i, p_i. In other words, $\mathcal{A}_{i,s(i)}(p_i) \subseteq \mathcal{F}_{s(i)} \subseteq \mathcal{D}$ such that $p_i \in \mathcal{A}_{i,s(i)}(p_i)$. Note that the initial position of every robot is assumed to be within its accessible domain. In Fig. 3, although both robots are rabbits, the accessible domain of Robot i is $\mathcal{A}_{i,s(i)}(p_i) = \mathcal{D}_{1,1}$ whereas that of Robot j is $\mathcal{A}_{j,s(j)}(p_j) = \mathcal{D}_{1,2}$. On the other hand, the accessible domains of the three turtle robots in the same figure are identical as $\mathcal{A}_{k,s(k)}(p_k) = \mathcal{A}_{l,s(l)}(p_l) = \mathcal{A}_{m,s(m)}(p_m) = \mathcal{D}$ which is the whole domain.

In case of covering a domain that consists of multiple types of terrains (subdomains) with a team of robots with different mobility types, the traditional Voronoi tessellation may end up assigning inaccessible regions to some of the robots because it only considers the distance between a point and a robot. This may cause the center of mass of a robot's Voronoi cell to be outside of the robot's accessible domain, and a gradient descent controller can drive the robot into its incompatible regions. Also, if the purpose of the coverage is not sensing but servicing of events which require the robots to visit any points within their Voronoi cells, the Voronoi cells should only contain the accessible domains of the robots.

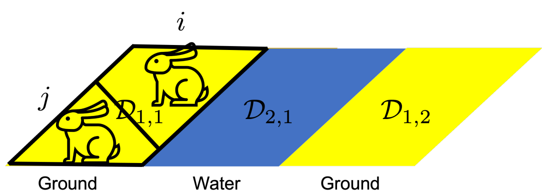

Fig. 4. An example of mobility constrained Voronoi tessellation with two rabbit robots with accessible domain $\mathcal{D}_{1,1}$.

Therefore, we define a mobility constrained Voronoi cell of the i^{th} robot as

$$V_{i,s(i)}(p) = \{q \in \mathcal{A}_{i,s(i)}(p_i) | \|q - p_i\| \le \|q - p_j\|, \forall j \in \mathcal{N}\}.$$

Note that the mobility constrained Voronoi cell of a robot is confined to the accessible domain of the robot. An example of the mobility constrained Voronoi cells is shown in Fig. 4. Since two rabbit robots i and j are on $\mathcal{D}_{1,1}$ in the figure, their Voronoi cells are confined to the connected subdomain $\mathcal{D}_{1,1}$.

III. Mobility Constrained Locational Cost and Gradient Descent Algorithm

The quality of the coverage performed by a multi-robot team over a domain of interest can be quantified with a locational cost. Since the region of dominance of a robot is redefined as the mobility constrained Voronoi cell in the previous section, the locational cost also needs to be reformulated. We call the new locational cost of the system as the mobility constrained locational cost. The mobility constrained locational cost of the Robot i is given as

$$\mathcal{H}_{m,i}(p) = \int_{V_{i,s(i)}(p)} \|q - p_i\|^2 \phi(q) dq$$

where $\phi : \mathcal{D} \to \mathbb{R}_{\ge 0}$ is a density function that describes the importance of a point q. The mobility constrained locational cost of the multi-robot system can be obtained by summing the costs of all robots as

$$\mathcal{H}_m(p) = \sum_{i=1}^{n} \int_{V_{i,s(i)}(p)} \|q - p_i\|^2 \phi(q) dq. \tag{1}$$

Note that the only difference between the mobility constrained locational cost and the traditional locational cost is the definition of the Voronoi cell.

A heterogeneous team of robots with different mobility types can achieve an optimal coverage over a domain by minimizing the mobility constrained locational cost in (1). One way to achieve this is letting each robot move against the gradient of the cost with respect to its position, which eventually makes the robots converge to local minimizers. For this, the gradient of the mobility constrained locational cost with respect to a robot's position needs to be calculated.

Note that the mobility constrained locational cost in (1) is the summation of the cost of every robot. Since only the costs of Robot i and its direct neighbors depend on p_i, taking partial derivative of the cost function in (1) with respect to p_i gives

$$\begin{aligned} \frac{\partial \mathcal{H}_m(p)}{\partial p_i} &= \frac{\partial}{\partial p_i} \int_{V_{i,s(i)}(p)} \|q - p_i\|^2 \phi(q) dq \\ &\quad + \frac{\partial}{\partial p_i} \sum_{j \in \mathcal{N}_i} \int_{V_{j,s(j)}(p)} \|q - p_j\|^2 \phi(q) dq \end{aligned} \tag{2}$$

where $\mathcal{N}_i$ represents the Delaunay neighbors of Robot i. Here, Delaunay neighbors indicate the robots that share a boundary. In order to compute the partial derivative, we need to apply Leibniz integral rule.

Lemma 1. *(Leibniz Integral Rule [22]) Let $\Omega(p)$ be a region that depends smoothly on p such that the unit outward normal vector n(p) is uniquely defined almost everywhere on the boundary $\partial\Omega(p)$. Let*

$$F = \int_{\Omega(p)} f(p, q) dq.$$

Then,

$$\frac{\partial F}{\partial p} = \int_{\Omega(p)} \frac{\partial}{\partial p} f(p, q) dq + \int_{\partial\Omega(p)} f(p, q) n(q)^\top \frac{\partial q}{\partial p} dq$$

where the second term is the line integral over the boundary, $\partial\Omega(p)$.

Applying Lemma 1 to (2) and simplifying terms, we get

$$\begin{aligned} \frac{\partial \mathcal{H}_m(p)}{\partial p_i} &= 2 \int_{V_{i,s(i)}(p)} (p_i - q)^\top \phi(q) dq \\ &\quad + \sum_{j \in \mathcal{N}_i} \int_{\partial V_{ij}(p)} \|q - p_i\|^2 n_i(q)^\top \frac{\partial q}{\partial p_i} dq \\ &\quad + \sum_{j \in \mathcal{N}_i} \int_{\partial V_{ij}(p)} \|q - p_j\|^2 n_j(q)^\top \frac{\partial q}{\partial p_i} dq \end{aligned}$$

where $\partial V_{ij}(p)$ is the boundary between Voronoi cells i and j. Since $n_i(q) = -n_j(q)$ and $\|q - p_i\| = \|q - p_j\|$ along the boundaries of the neighboring Voronoi cells i and j, $\partial V_{ij}(p)$, the summation terms become 0. Therefore, the gradient of the mobility constrained locational cost is given as

$$\frac{\partial \mathcal{H}_m(p)}{\partial p_i} = 2\int_{V_{i,s(i)}} (p_i - q)^\top \phi(q)dq$$

where the dependence of p on the mobility constrained Voronoi cell is omitted for notational convenience. Substituting the mass and the center of mass of the mobility constrained Voronoi cell,

$$m_{i,s(i)}(p) = \int_{V_{i,s(i)}} \phi(q)dq, \;\; c_{i,s(i)}(p) = \frac{\int_{V_{i,s(i)}} q\phi(q)dq}{m_{i,s_i}(p)},$$

into the gradient expression, we finally get

$$\frac{\partial \mathcal{H}_m(p)}{\partial p_i} = 2m_{i,s(i)}(p)\left(p_i - c_{i,s(i)}(p)\right)^\top$$

which is fundamentally in the same form as the gradient in the homogeneous case [2], except for the definitions of the mass and the center of mass of the Voronoi cells.

Assuming the robots are single integrators, $\dot{p}_i = u_i$, the gradient descent controller for Robot i is given as

$$u_i = -\frac{\partial \mathcal{H}_m(p)}{\partial p_i}^\top = -2m_{i,s(i)}(p)\left(p_i - c_{i,s(i)}(p)\right).$$

We can now scale the control signal with a positive gain $\gamma_i(p) = \frac{k_i}{2m_{i,s(i)}(p)} > 0$ with $k_i \in \mathbb{R}_{\geq 0}$, which simplifies the controller to

$$u_i = -k_i\left(p_i - c_{i,s(i)}(p)\right). \tag{3}$$

The convergence of the robots under the control law in (3) can be checked by analyzing the time derivative of the mobility constrained locational cost, which is calculated as

$$\dot{\mathcal{H}}_m(p) = \frac{\partial \mathcal{H}_m(p)}{\partial p}\dot{p} = -\sum_{i=1}^{n}\gamma_i(p)\left\|\frac{\partial \mathcal{H}_m(p)}{\partial p_i}^\top\right\|^2$$

where $\gamma_i(p)$ is the gain of the i^{th} robot defined above. Since the largest invariant set of p for $\mathcal{H}_m(p)$ is equal to the equilibrium of the system, by Lasalle's invariance principle, $p_i \to c_{i,s(i)}(p), \; \forall i \in \mathcal{N}$ as $t \to \infty$.

IV. Control Barrier Functions for Safe Heterogeneous Coverage

The gradient descent controller from the previous section drives each robot towards the center of mass of its mobility constrained Voronoi cell to achieve an optimal coverage configuration. Therefore, if the center of mass of every mobility constrained Voronoi cell is always within the cell, the gradient descent controller can serve as the safe coverage controller that keeps each robot within its accessible domain since $V_{i,s(i)}(p) \subseteq \mathcal{A}_{i,s(i)}(p_i)$. However, the accessible domains defined in Section II are not necessarily convex. Thus, the mobility constrained Voronoi cell of the robot can be non-convex as well. In this case, the center of mass of the mobility constrained Voronoi cell of a robot can be outside the cell depending on the density function applied on the domain. Therefore, it is possible for the gradient descent controller in (3) to drive robots into their inaccessible regions, which may lead to loss of functionality of those robots. In order to prevent such situations, control barrier functions (CBFs) [21] are utilized based on the property that CBFs ensure a system to remain in its safe set if it starts from the set.

In general, for control-affine robots, the dynamics of Robot i can be given by

$$\dot{p}_i = f(p_i) + g(p_i)u_i$$

where f and g are locally Lipschits, and $u_i \in U \subset \mathbb{R}^m$ is an admissable control input. Since we previously assumed that the robots are single integrators, we can represent the robot dynamics in control-affine form by letting $f(p_i) = 0$ and $g(p_i) = I_{2\times 2}$ for all $p_i \in \mathcal{D}$ where $I_{2\times 2}$ is a 2×2 identity matrix. Now, let $h_i(p_i)$ be a continuously differentiable function that defines the accessible domain (safe set) of Robot i in species $s(i)$ as below

$$\mathcal{A}_{i,s(i)}(p_i) = \{p_i \in \mathcal{D} \subset \mathbb{R}^2 | h_i(p_i) \geq 0\}.$$

Then, the function $h_i(p_i)$ is a control barrier function (CBF) if there exists an extended class $\mathcal{K}_\infty$ function α that satisfies

$$\sup_{u_i \in U}\left[L_f h_i(p_i) + L_g h_i(p_i)u_i\right] \geq -\alpha(h_i(p_i))$$

for all $p_i \in \mathcal{D}$. If $h_i(p_i)$ is a CBF, Robot i can be kept within its accessible domain, the safe set of Robot i [21].

However, it might not be feasible to represent the accessible domain of a robot as a superlevel set of a single continuously differentiable function if the shape of the domain is complex. Therefore, we introduce the following assumption.

Assumption 1. *The accessible domains of the robots can be represented by the intersection of a finite number of superlevel sets of continuously differentiable functions.*

Even in cases where it is impossible to exactly represent the accessible domain of a robot as in Assumption 1, we can always under-approximate the domain with continuously differentiable functions to obtain a conservative and safe representation of the domain.

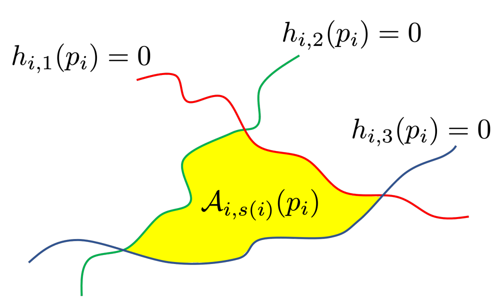

Fig. 5. An example illustrating Assumption 1 for Robot i with 3 constraints. The yellow area indicates the accessible domain of Robot i.

If Assumption 1 holds, according to [23], the logical *and* of the constraints that altogether define the accessible domain of a robot, $h_i(p_i) = h_{i,1}(p_i) \wedge h_{i,2}(p_i) \wedge \cdots \wedge h_{i,l_i}(p_i)$, can be compressed into

$$h_i(p_i) = \min_{z \in L_i} \{h_{i,z}(p_i)\}$$

where $l_i = con(A_{i,s(i)}(p_i))$ is the total number of constraints of Robot i, and $L_i = \{1, \cdots, l_i\}$ is the set of indices of the constraints of Robot i.

Finally, letting $\hat{u}_i$ be the gradient descent controller derived in (3), we can consider the following Quadratic Programming (QP) controller similar to the one devised in [24]

$$\begin{aligned} u^* = \arg\min_u \sum_{i=1}^{n} \|u_i - \hat{u_i}\|^2 \\ s.t.\ L_f h_i(p_i) + L_g h_i(p_i) u_i \geq -\alpha(h_i(p_i))\ \forall i \in \mathcal{N} \end{aligned} \tag{4}$$

which is the minimally invasive coverage controller that drives each robot towards the weighted centroid of its mobility constrained Voronoi cell while keeping the robot within its accessible region. Here, $u = [u_1^\top, \cdots, u_n^\top]^\top$.

V. Experimental Results

In this section, the effectiveness of the safe heterogeneous controller in (4) is demonstrated in two different setups. In both cases, a group of heterogeneous robots consisting of ground and amphibious robots is used, and we denote ground robots as rabbits and amphibious robots as turtles. The experiments were performed in the Robotarium [25], a remotely accessible multi-robot research testbed. In the Robotarium, the rectangular boundary for the robots is defined as $[-1.6, 1.6]$ for the x-axis and $[-1, 1]$ for the y-axis where each axis has unit of meters. The density function used in the experiments is a bivariate normal distribution defined as

$$\phi(q) = \frac{1}{2\pi\sqrt{|\Sigma|}} e^{-\frac{1}{2}(q-\mu)^\top \Sigma^{-1}(q-\mu)} \tag{5}$$

where μ is the mean, and Σ is the covariance matrix of the distribution. Specifically, those values are set to $\mu = [0, 0]^\top$ and $\Sigma = 0.3 I_{2\times2}$ with $I_{2\times2}$ being the 2×2 identity matrix.

In the first experiment, a simple multi-terrain domain described in Fig. 6a was used. The left half plane in dark blue in the figure represent water region, and the right half plane in light blue represent ground region. Also, the density function (5) is visualized with a gradation of colors which is overlaid on the domain. All of the robots start from the ground subdomain, so the accessible domain for all rabbits are the right half plane defined as $x \geq 0$. If we let $\mathcal{S} = \{1, 2\}$ with $1 \in \mathcal{S}$ representing rabbits and $2 \in \mathcal{S}$ representing turtles, the barrier function for rabbits is given as $h_i(p_i) = p_{i,x},\ \forall \{i \in \mathcal{N} | s(i) = 1\}$ where $p_{i,x}$ is the x-component of the position vector of Robot i, p_i. On the other hand, since the accessible domain of the turtle robots is the whole domain $\mathcal{D}$, the barrier function for turtles is simply given as $h_i(p_i) = 0,\ \forall \{i \in \mathcal{N} | s(i) = 2\}$. For the experiment, $\alpha(h_i(p_i))$ in (4) was chosen to be $100 h_i(p_i)^3$. From Fig. 6b, it can be confirmed that the rabbits never left the ground whereas the turtles moved into water to obtain better coverage. The evolution of the cost function for this experiment is shown in Fig. 6c.

For another experiment, a multi-terrain domain similar to the one in Fig. 1 with two ground connected subdomains and one water subdomain was used. In this case, however, two connected subdomains are non-convex as shown in Fig. 7a. The left ground subdomain is defined as $2x^2 - y^2 - 1 \geq 0$ where $x < 0$, and the the right ground subdomain is defined as the intersection of $x + y^2 - 1 \geq 0$ and $x + y - 0.7 \geq 0$. Therefore, there is only one barrier function defined as $2p_{i,x}^2 - p_{i,y}^2 - 1 = 0$ for rabbits starting from the left ground subdomain where $p_{i,x}$ and $p_{i,y}$ represent the x and y coordinates of the Robot i, respectively. In contrast, there are two barrier functions defined as $p_{i,x} + p_{i,y}^2 - 1 = 0$ and $p_{i,x} + p_{i,y} - 0.7 = 0$ for rabbits starting from the right ground subdomain. Like in the first experiment, the barrier function for turtles is trivially given as $h_i(p_i) = 0,\ \forall \{i \in \mathcal{N} | s(i) = 2\}$. In the experiment, $\alpha(h_i(p_i)) = 100 h_i(p_i)^3$ was used. From Fig. 7b, it can be confirmed that rabbits never left ground subdomains while moving into higher density regions. The evolution of the cost function for this experiment is described in Fig. 7c.

VI. CONCLUSIONS

In this paper, we proposed a coverage control strategy for multi-terrain and multi-species scenarios. In such cases, robots with different mobility types have different compatible regions throughout the multi-terrain domain. Therefore, the safe operating regions of a robot is determined based on its species and current position. In this work, the problem of coverage is considered as the combination of sensing and potential servicing of an event that might need a robot to visit locations within its region of dominance. Therefore, the Voronoi cell of a robot is confined to the robot's accessible regions, and the new locational cost is defined based on the new Voronoi cells. In order to achieve an optimal coverage under the cost, each robot is driven by a gradient descent controller. In addition, control barrier functions are utilized to keep robots within their accessible domains even if the domains are non-convex. Experimental results show that the proposed strategy achieves an optimal coverage over a domain while keeping every robot in its safe region.

References

[1] J. Cortes and M. Egerstedt, "Coordinated control of multi-robot systems: A survey," *SICE Journal of Control, Measurement, and System Integration*, vol. 10, no. 6, pp. 495–503, 2017.

[2] J. Cortes, S. Martinez, T. Karatas, and F. Bullo, "Coverage control for mobile sensing networks," *IEEE Transactions on Robotics and Automation*, vol. 20, no. 2, pp. 243–255, 2004.

[3] S. Lloyd, "Least squares quantization in pcm," *IEEE Transactions on Information Theory*, vol. 28, no. 2, pp. 129–137, 1982.

[4] A. Okabe, B. Boots, K. Sugihara, and S. N. Chiu, *Spatial Tessellations: Concepts and Applications of Voronoi Diagrams*. New York, NY, USA: John Wiley & Sons, Inc., 2000.

[5] L. C. A. Pimenta, V. Kumar, R. C. Mesquita, and G. A. S. Pereira, "Sensing and coverage for a network of heterogeneous robots," in *2008 47th IEEE Conference on Decision and Control*, 2008, pp. 3947–3952.

[6] A. Pierson, L. C. Figueiredo, L. C. A. Pimenta, and M. Schwager, "Adapting to performance variations in multi-robot coverage," in *2015 IEEE International Conference on Robotics and Automation (ICRA)*, 2015, pp. 415–420.

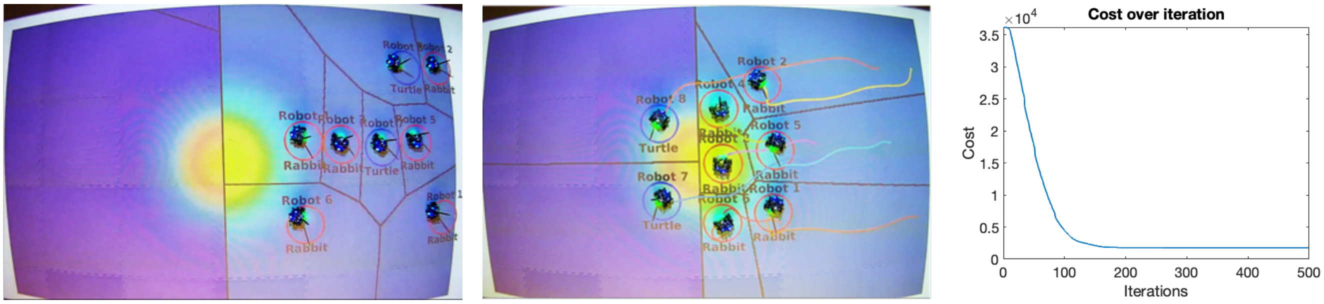

(a) Initial Configuration (b) Final Configuration (c) Evolution of the Cost Function

Fig. 6. (a) Initial configuration of a robot team consisting of rabbits (ground robots) and turtles (amphibious robots) on a domain with convex subdomains. Rabbits and turtles are indicated with red and blue circles around them, respectively. The left half plane in dark blue is water subdomain, and the right half plane in light blue is ground subdomain. The density function is visualized with a gradation of colors where colors close to yellow indicate higher density, and colors close to blue indicate lower density. (b) The final positions and trajectories of the robots running (4) with the initial conditions in Fig. 6a. (c) Evolution of the cost function over iterations.

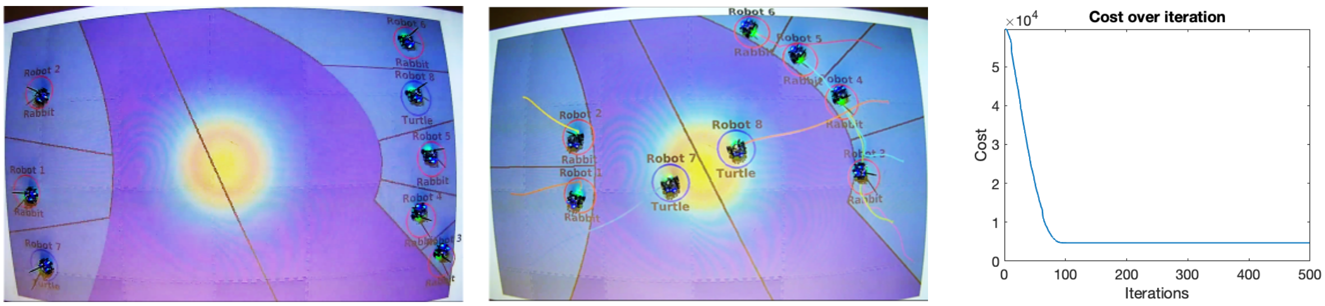

(a) Initial Configuration (b) Final Configuration (c) Evolution of the Cost Function

Fig. 7. (a) Initial configuration of a robot team on a domain with non-convex subdomains. The regions in light blue and the region in dark blue represent ground and water subdomains, respectively. (b) The final positions and trajectories of the robots running (4) with the initial conditions in Fig. 7a. (c) Evolution of the cost function over iterations.

[7] H. Mahboubi, K. Moezzi, A. G. Aghdam, K. Sayrafian-Pour, and V. Marbukh, "Self-deployment algorithms for coverage problem in a network of mobile sensors with unidentical sensing ranges," in *2010 IEEE Global Telecommunications Conference GLOBECOM 2010*, 2010, pp. 1–6.

[8] M. Santos, Y. Diaz-Mercado, and M. Egerstedt, "Coverage control for multirobot teams with heterogeneous sensing capabilities," *IEEE Robotics and Automation Letters*, vol. 3, no. 2, pp. 919–925, 2018.

[9] M. Santos and M. Egerstedt, "Coverage control for multi-robot teams with heterogeneous sensing capabilities using limited communications," in *2018 IEEE/RSJ International Conference on Intelligent Robots and Systems (IROS)*, 2018, pp. 5313–5319.

[10] A. Sadeghi and S. L. Smith, "Coverage control for multiple event types with heterogeneous robots," in *2019 International Conference on Robotics and Automation (ICRA)*, 2019, pp. 3377–3383.

[11] A. Pierson, L. C. Figueiredo, L. C. Pimenta, and M. Schwager, "Adapting to sensing and actuation variations in multi-robot coverage," *The International Journal of Robotics Research*, vol. 36, no. 3, pp. 337–354, 2017.

[12] J. Zhang, P. Zhou, and L. Ma, "Coverage control of multiple heterogeneous mobile robots with nonholonomic constraints," in *2016 35th Chinese Control Conference (CCC)*, 2016, pp. 6272–6277.

[13] M. S. Miah and J. Knoll, "Area coverage optimization using heterogeneous robots: Algorithm and implementation," *IEEE Transactions on Instrumentation and Measurement*, vol. 67, no. 6, pp. 1380–1388, 2018.

[14] A. Kwok and S. Martinez, "Deployment algorithms for a power-constrained mobile sensor network," in *2008 IEEE International Conference on Robotics and Automation*, 2008, pp. 140–145.

[15] O. Arslan and D. E. Koditschek, "Voronoi-based coverage control of heterogeneous disk-shaped robots," in *2016 IEEE International Conference on Robotics and Automation (ICRA)*, 2016, pp. 4259–4266.

[16] H. Mahboubi, F. Sharifi, A. G. Aghdam, and Y. Zhang, "Distributed coordination of multi-agent systems for coverage problem in presence of obstacles," in *2012 American Control Conference (ACC)*, 2012, pp. 5252–5257.

[17] M. Adibi, H. A. Talebi, and K. Y. Nikravesh, "Adaptive coverage control in non-convex environments with unknown obstacles," in *2013 21st Iranian Conference on Electrical Engineering (ICEE)*, 2013, pp. 1–6.

[18] J. M. Palacios-Gasós, Z. Talebpour, E. Montijano, C. Sagüés, and A. Martinoli, "Optimal path planning and coverage control for multi-robot persistent coverage in environments with obstacles," in *2017 IEEE International Conference on Robotics and Automation (ICRA)*, 2017, pp. 1321–1327.

[19] A. Mellone, G. Franzini, L. Pollini, and M. Innocenti, "Persistent coverage control for teams of heterogeneous agents," in *2018 IEEE Conference on Decision and Control (CDC)*, 2018, pp. 2114–2119.

[20] N. Boonpinon and A. Sudsang, "Constrained coverage for heterogeneous multi-robot team," in *2007 IEEE International Conference on Robotics and Biomimetics (ROBIO)*, 2007, pp. 799–804.

[21] A. D. Ames, S. Coogan, M. Egerstedt, G. Notomista, K. Sreenath, and P. Tabuada, "Control barrier functions: Theory and applications," in *2019 18th European Control Conference (ECC)*, 2019, pp. 3420–3431.

[22] Q. Du, V. Faber, and M. Gunzburger, "Centroidal voronoi tessellations: Applications and algorithms," *SIAM Review*, vol. 41, no. 4, pp. 637–676, 1999.

[23] P. Glotfelter, J. Cortés, and M. Egerstedt, "Nonsmooth barrier functions with applications to multi-robot systems," *IEEE Control Systems Letters*, vol. 1, no. 2, pp. 310–315, 2017.

[24] A. D. Ames, X. Xu, J. W. Grizzle, and P. Tabuada, "Control barrier function based quadratic programs for safety critical systems," *IEEE Transactions on Automatic Control*, vol. 62, no. 8, pp. 3861–3876, 2017.

[25] S. Wilson, P. Glotfelter, L. Wang, S. Mayya, G. Notomista, M. Mote, and M. Egerstedt, "The robotarium: Globally impactful opportunities, challenges, and lessons learned in remote-access, distributed control of multirobot systems," *IEEE Control Systems Magazine*, vol. 40, no. 1, pp. 26–44, 2020.